Desalination 286 (2012) 429–435

Contents lists available at SciVerse ScienceDirect

Desalination

journal homepage: www.elsevier.com/locate/desal

Low-cost monofilament mesh filter used in membrane bioreactor process: Filtration characteristics and resistance analysis

Amir Ali Poostchi, Mohammad Reza Mehrnia *, Fariba Rezvani, Mohammad Hossein Sarrafzadeh

Biotechnology Group, School of Chemical Engineering, College of Engineering, University of Tehran, P.O. Box 11155-4563, Tehran, Iran

ARTICLE INFO

Article history:
Received 14 September 2011
Received in revised form 4 December 2011
Accepted 6 December 2011
Available online 4 January 2012

Keywords:
Mesh filter
Membrane bioreactor
Filtration characteristics
Resistance

ABSTRACT

This work investigates filtration performance of mesh filter bioreactor for synthetic municipal wastewater treatment. Critical flux is measured by flux stepping method and the effect of aeration rate on the critical flux is investigated. The long term monitoring of trans-filter pressure evolution at sub and super-critical fluxes is performed. The analysis of resistance is achieved by determination of resistances and microscopic observation of bio-cake. Cake resistance values vary from 78% to 92% of total filtration resistance for sub and super-critical fluxes. The effect of variations of specific aeration demands (SAD_m: 0.5–6 m^3/m^2 h) on suspended solid of effluent, turbidity of filtrate, filtration resistance, and zeta potential of biomass is evaluated. The results show that filtrate quality is decreased when the aeration rate increases. It is attributed to stable formation of dynamic membrane. A rather clear filtrate, less than 18 NTU of turbidity, is obtained for SAD_m 0.5 m^3/m^2 h. The results also show that the total filtration resistance of the sub-critical flux significantly decreases with increasing aeration intensity until SAD_m 2 m^3/m^2 h and thereafter slightly decreases. It is also shown that the variations of zeta potential of biomass with aeration rate highly correspond to the alterations of filtration resistance.

1. Introduction

Membrane bioreactor (MBR) is an important liquid–solid separation technology and an option of choice which has been extensively employed in the wastewater treatment [1,2]. MBRs offer two main advantages including a significantly improved effluent quality; due to high mixed liquor suspended solid (MLSS) concentration, and a substantially small footprint; due to absence of secondary settling tank [3–6]. So far, unavoidable membrane fouling and the high cost of membranes are major obstacles to the wide application of MBRs [7]. In recent years, there are considerable investigations focusing on development of possibly efficient procedures to mitigate the fouling of membrane in MBRs [8,9]. In this context, using low-cost filter materials including woven and non-woven can be considered as the suitable alternatives to the conventional membrane which offer higher flux rates at lower trans-membrane pressures. Kiso et al. [10] studied the performance of mesh filtration bioreactor which was equipped with a nylon mesh filter as filter material instead of microfiltration membrane in a MBR. They examined the use of meshes as coarser filter material with three pore sizes 100, 200, and 500 μm for activated sludge separation and found that a mesh with pore size of 100 μm effectively rejected activated sludge. They also investigated the performance of combined process of sequencing batch reactor and mesh filtration bioreactor [11]. Fuchs et al. [12] investigated the influence of operational conditions such as suspended solid concentration, flux rate and aeration rate on the performance of a mesh filter in the activated sludge process. The main results showed that the mesh filtration process was effective under different operation conditions. Chang et al. [13] conducted the experimental studies to investigate the performance and filtration characteristics of a non-woven filter submerged in membrane bioreactor for synthetic wastewater treatment. The filter was made of polypropylene and the surface of the filter modified by use of plasma technique. Ren et al. [14] used a non-woven polyester fabric filter with 100 μm nominal pore size in a MBR to treat household wastewater. Zahid and El-Shafai [15] evaluated the performance of cloth-media filters made of three materials (Acrylate, Polyester, and Nylon) for MBR treating municipal wastewater. They found that three used filter materials were effective in removing 99% of total suspended solids and turbidity. Compared to a numerous studies on micro and ultrafiltration membranes for MBR wastewater treatment, limited information about filtration process is obtained from the literature regarding the use of filter media in the MBR systems. As mentioned above, most of the studies focused on the performance of synthetic fabric materials for treatment of several sources of wastewater. But, there are very few investigations on operational characteristics and filtration performance of woven and non-woven filters as basic mechanisms of filtration of micro and ultrafiltration membranes are not comparable to depth filtration of fabric filters.

In this work, the monofilament mesh filter made of polyester fabric is used with 30 μm average pore size. In order to investigate the filtration aspects of the mesh, the critical flux determination and

* Corresponding author. Tel.: +98 21 61112184; fax: +98 21 66954041.
E-mail address: mmehrnia@ut.ac.ir (M.R. Mehrnia).

0011-9164/$ – see front matter © 2011 Elsevier B.V. All rights reserved.
doi:10.1016/j.desal.2011.12.002

regular flux and trans-filter pressure measurements are performed. Since the filtration resistance is very significant for understanding of filtration extent, the filtration resistance analysis of the mesh is performed while the trans-filter pressure is developed during time of operation. Aeration intensity is recognized as a key operational parameter in MBRs, influencing the effluent quality and filtration performance. The critical issues are the formation of a sludge layer acting as the actual membrane filter and the accumulation of the excess sludge leading to rapid increase in the filtration resistance. In this work, the effect of aeration intensity on the filtrate quality and filtration resistance is also investigated in order to evaluate the appropriate aeration intensities to meet the optimum filtration conditions. Moreover, the variations of biomass characteristic such as zeta potential with aeration intensity are also studied.

2. Material and methods

2.1. Experimental set up

The schematic process flow diagram of experimental setup is illustrated in Fig. 1(a). The filtration tests are carried out in a rectangular Plexiglas vessel with a 0.15 m width, 0.2 m length and 0.4 m height. The monofilament mesh filter made of polyester is used with average pore size 30 μm. The resulting effective area is 156 cm^2 or roughly 0.016 m^2. A rectangular holding frame made of polyethylene is constructed to tightly support mesh filter. To avoid leakage, a neoprene gasket is used to strictly seal the sides of mesh filter. The filter medium with its holding frame, as shown in Fig. 1(b), is vertically submerged in a center of bioreactor. A nozzle is mounted on the body of the holding frame to conduct filtrate flow toward a permeate tube. The pressure drop across the filter medium is measured by a high precision pressure transducer installed in the filtrate line as close as possible to the filter module. The sensor is connected to the on-board controller and analog to digital card (I/O module) in order to transmit the digital signals to a PC for data gathering and acquisition. Data is collected every 5 s and recorded on dedicated log sheets during the experiments. A dedicated module of MATLAB software is used to filter the large amount of input data of trans-filter pressures (TFP). A peristaltic pump which operates at a preset flow rate is used to suck the treated flow through mesh filter and subsequently to transfer the effluent to a treated tank. The rate of effluent is timely monitored by the use of a calibrated flow meter. The bioreactor is equipped with five air pipe spargers evenly installed at the bottom of the bioreactor; one of which is exactly placed below the filter module for intermittent cleaning of filter surface. The rate of sparging aeration is monitored by the use of a calibrated rotameter. Clean air supplied by a blower is passed through an air manifold mounted on the top of the bioreactor. The air flow is separately distributed into five parallel tubes mounted on the inner side wall of the bioreactor in such a way that it can be removed. The air flow rate of each pipe sparger is regulated by automatic control valve independently installed in the air manifold. The pipe sparger has a 0.04 m inner diameter generating fine bubbles. It has forty evenly space orifices symmetrically drilled on its top, bottom and side surface.

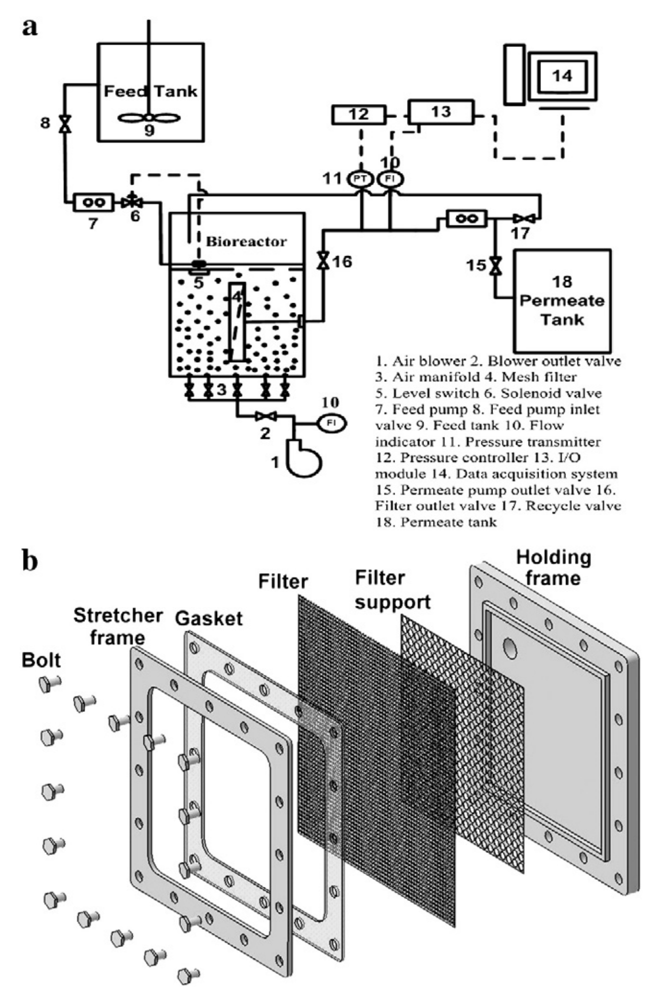

Fig. 1. (a) Process flow diagram of mesh filter bioreactor system; (b) sketch of mesh filter module.

2.2. Operation conditions of continuous bioreactor

The working volume of the bioreactor is 6 L. The aeration rate varies between 0.13 and 1.6 L/min and the dissolved oxygen concentrations are in the range of 3.4–5.6 mg/L. The bioreactor temperature is set in the range of 23–25 °C as the temperature fluctuation affects the performance of activated sludge. The hydraulic retention time (HRT) is set between 4.7 and 12.5 h corresponding to preset flow rates. With removing a specific amount of biomass from bioreactor, sludge residence time (SRT) is kept at 33.4 days. MLSS concentration is kept almost constant between 6.1 and 8.7 g/L by withdrawing the additional amount of biomass from bioreactor. Fig. 2 shows the MLSS and the VSS/MLSS values. The bioreactor operates with synthetic glucose based wastewater. The influent contains 450 mg/L glucose, 92.7 mg/L ammonium sulfate, and 20.4 mg/L ammonium phosphate. The COD:N:P ratio in the wastewater is about 100:5:1. $NaHCO_3$ is used as a buffer to adjust pH to 7. Required trace metals derived from $CaCl_2$, $MgSO_4$, $FeSO_4$, and $MnSO_4$ are provided to the system.

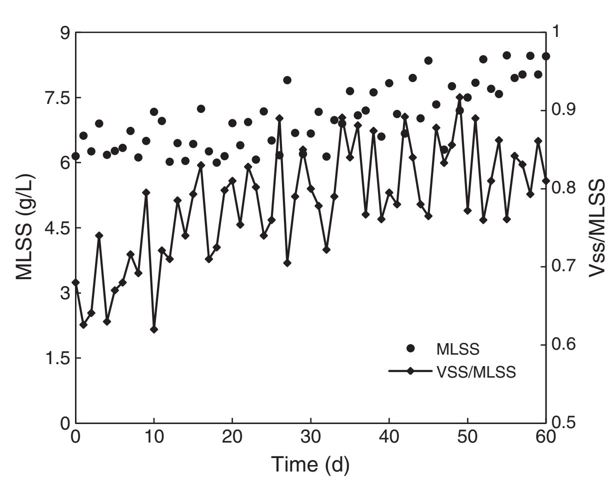

Fig. 2. MLSS profile in continuous mesh filter bioreactor.

Seed sludge is taken from the operating MBR plant (installed by Huber technology), dedicated for treating municipal wastewater. The sludge suspensions are acclimatized for 105 days with the same operating parameters of the MBR. After that, the sludge suspension is loaded to the MBR with the MLSS concentration of 6 g/L.

2.3. Analytical procedures

The turbidity of the filtrate flow is determined by the use of spectrophotometer (Spectroquant *Multy*, Merck, Germany). MLSS concentration and corresponding volatile suspended solids (VSS) are measured using standard method 2540 [16]. Dissolved oxygen is measured using DO meter (WTW 340 *i*, Germany). The zeta potential of sludge is measured by the use of *Zeta Plus* model (Brookhaven, US).

2.4. Field emission scanning electron microscopic (FESEM)

The surface of fresh mesh filter and surface of cake layer formed on the used mesh filter with corresponding cross-section structure is observed with the help of a scanning electron microscopy (S4160, Hitachi, Japan). The height of cake layer is characterized easily as the boundary between the filter and the cake is readily distinguishable. When the complete formation of bio-cake layer is done, the suction pump is stopped and the permeate valve is normally closed to prevent the back flow of the filtrate due to driving force owing to relatively high pressure difference between filter module and suction line. The filter with the deposited layer of sludge particles is separated from the holding frame. The sample is fixed with 2% (v/v) glutaraldehyde in 0.1 M phosphate buffer at pH 7.2 for 2 h and then washed for 10 min and again immersed for 1 h in 0.1 M phosphate buffer. The sample is dehydrated with ethanol. When the drying is accomplished, the sample of bio-cake is precisely obtained and accurately fixed to the welfare of SEM. Especial attention shall be attained when the specimen of cake layer is separated and put on the surface of welfare for preserving the origin of microstructure. A coating of gold by a sputter is set on the sample for increasing surface resolution.

2.5. Filtration resistance analysis

The filter fouling phenomenon can be described by using a theoretical model known as the resistance-in-series model [17–19]:

$$J = \frac{\Delta P}{\mu R_t} \tag{1}$$

$$R_t = R_m + R_c + R_f \tag{2}$$

where J is the permeate flux (m^3/m^2s), ΔP the trans-filter pressure (Pa), μ the viscosity of permeate (Pa.s), R_t the total filtration resistance (1/m), R_m the filter resistance (1/m), R_c the cake resistance caused by the cake layer deposited over the filter surface (1/m), R_f the fouling resistance caused by pore blocking and irreversible adsorption of foulants onto the filter pore wall or surface (1/m). The mentioned resistances are calculated using the following equations:

$$R_m = \frac{\Delta P}{\mu J_w} \tag{3}$$

$$R_f = \frac{\Delta P}{\mu J_{wf}} - R_m \tag{4}$$

$$R_c = \frac{\Delta P}{\mu J_{AS}} - R_m - R_f \tag{5}$$

where J_w is the initial tap water flux, J_{wf} the final tap water flux after removing the cake layer by flushing with tap water and J_{AS} is the flux of activated sludge at steady state [20].

3. Result and discussions

3.1. Critical flux of mesh filter

The beneficial effect of using mesh filter in MBR is that the filter is able to remarkably increase the sustainable flux of MBR, compared to conventional micro and ultrafiltration membrane of MBR. The concept of critical flux is introduced as convenient criteria to predict fouling [21]. Critical flux is defined as a flux below which fouling is absent or negligible. To optimize the operational conditions of a MBR system, it is necessary to determine the critical flux since it allows trading-off two operational issues, including on-stream factor and permeate flux without any chemical cleaning required. Determination of critical flux value is performed when the MLSS concentration of the bioreactor is stabilized at 6.1–8.7 g/L. Fresh monofilament mesh filter module is used for this purpose. The short-term flux-step method is used by increasing the flux in a stepwise mode and monitoring the TFP development. Wu et al. [22] investigated the effects of various factors on the critical flux. They reported that initial flux did not influence the critical flux, but step length and step height decreased and increased the critical flux value, respectively. Each run starts at a constant flux which is maintained for step length 20 min. If the TFP remains constant at the imposed flux, the flux is stepped up to the upper level by changing the revolution speed of suction pump. The initial constant flux is 35 L/m^2 h (LMH) and the step height of the imposed flux is set to 6 LMH. The procedure is repetitively performed till an obvious increase in the TFP is observed. Fig. 3 shows the flux and TFP profile obtained for monofilament mesh filter. As shown in Fig. 3, with the imposed flux between 35 and 71 LMH, there is no significant variation in the TFP and the TFP is almost constant. For polyester mesh, in the duration of 140 min the rate of TFP increase is still low and rises from 6 mbar to 12 mbar; in the subsequent 20 min, the rise is from 12 mbar to 26 mbar, when the TFP increases sensibly over 20 min, the consequently imposed flux is considered as critical flux. The critical flux is around 77 LMH with a standard deviation of 0.45. The effect of aeration intensity on the critical flux has also been investigated. Aeration imparted to the membrane is denoted SAD_m, the specific aeration demand in the volumetric rate of air per unit membrane area. Fig. 4 illustrates relation between the critical flux and SAD_m. As can be seen from Fig. 4, the critical flux value is increased when the rate of aeration increases. The mathematic equation of critical flux with specific aeration demand (SADm) is shown in Fig. 4 with R-squared value ($R^2 = 0.8859$). The critical flux is improved from 74 to 81 LMH with the SAD_m ranging from 0.5 to 6 m^3/m^2 h. The critical flux value is reproducible and dependent on the several

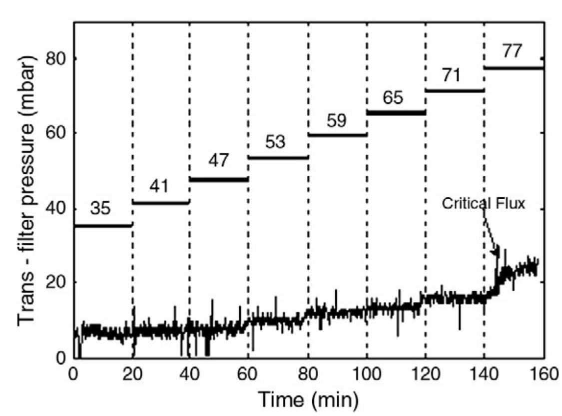

Fig. 3. Critical flux determination of continuous mesh filter.

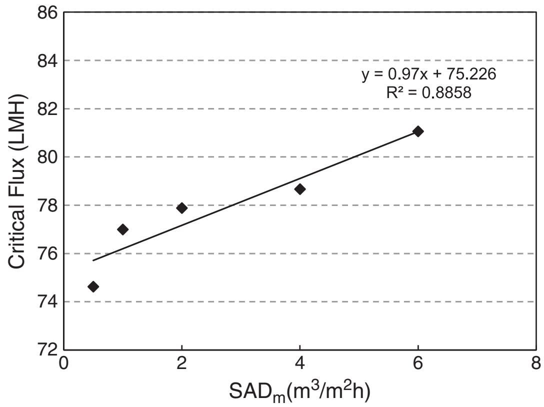

Fig. 4. Relationship between aeration intensity and critical flux.

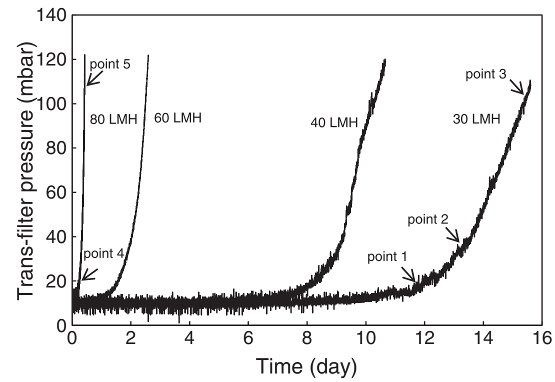

Fig. 5. TFP profile at various imposed fluxes.

factors, such as aeration intensity, initial imposed flux, step length and step height. Since characteristics of conventional membranes used in a MBR and the relative filtration mechanism are different in comparison with mesh filter, it cannot be rational to compare the critical flux of mesh with membrane media. On the other hand, the critical flux values for woven filters as well as monofilament mesh have rarely been reported in previous works. Tewari et al. [28] determined the critical flux for two filters, namely, nylon mesh and ash filter that was equal to 10 LMH and higher than 16 LMH, respectively. They also showed that at a lower MLSS concentration, critical flux increased several times compared to higher MLSS concentration. Table 1 presents the critical flux values for microfiltration membrane and depth filter used in a MBR with relative operational conditions.

3.2. Flux and TFP profile

Four flux values are considered to compare the TFP profiles at the imposed fluxes. The imposed fluxes are equal to 30, 40 and 60 LMH as the representatives of sub-critical fluxes and 80 LMH as the representative of super-critical flux. Fig. 5 depicts a comparison of the TFP profiles at four different values of the imposed flux. It is generally accepted when long-term operation of a MBR is carried out at sub-critical flux conditions, a new stage of the TFP increase is observed even for simple synthetic feeds. It has been indicated that the critical flux, especially determined by the flux-stepping approach, does not predict the stable permeability data for long-term operation of a MBR. However, the fouling rate is practically accepted to be much more sustainable at sub-critical operation. At first, the experiment run is performed for three imposed fluxes viz. 30, 40 and 60 LMH which are substantially lower than measured critical flux beforementioned. At the imposed fluxes 30 and 40 LMH, it is observed that the monofilament mesh establishes stable flux over the entire duration of 12 and 8 operation days, respectively. During this period of the filtration, no substantial change in the TFP is observed. It results that no fouling occurs at this duration and consequent cleaning is not required. However, after a period of 12 days, the TFP rises steeply to values as high as 100 mbar within 3–4 days. At this time, the mesh filter is taken from the bioreactor and cleaned with tap water. Then the mesh filter performance recovers obviously. For the imposed flux 60 LMH which is closer to the measured critical flux, the mesh filter displays no perceptible TFP increase over 2 days of the filtration. Although it is generally expected that the permeate flux below the critical flux leads to be stable, however, the data gathered from digital filtrate flow meter shows that the lowly sensible fluctuation for the imposed flux 60 LMH unpredictably occurs during the initial period of filtration. It may be attributed to the fact that as the imposed flux becomes closer to the critical flux, the alternatively unstable biomass-filter interactions occur. This fluctuation can be removed by setting up a relaxation at a short period in which the suction peristaltic pump is set off and no flow passes through the filter medium. In this circumstance, the continuous filtration combined with intermittent relaxation may allow the heterogeneously labile deposits to return back to the bioreactor due to the turbulence generated by air bubbling [30]. For the imposed flux 80 LMH, which is above the critical flux, the TFP is no longer stable and increases sharply that is the consequence of rapid accumulation of foulants. It is also observed that a decline of flux occurs while rise in the TFP happens. The TFP reaches 100 mbar during 8 h of filtration.

3.3. Filtration resistance analysis

The measurement of filtration resistance is of vital importance for understanding of filtration extent and/or for the optimization of

Table 1
Critical flux for microfiltration and depth filter.

Medium	Type	Pore size (μm)	Wastewater	MLSS (g/L)	Critical flux (LMH)	Aeration (L/min)	Reference
Membrane	Hollow fiber (PVDF)	0.2	Municipal wastewater	15–18	32–38	100	[23]
Membrane	Hollow fiber (PE)	0.4	Synthetic	7.5–8.2	27	–	[24]
Membrane	Hollow fiber (PVDF)	0.2	Synthetic	5.5	20	–	[25]
Membrane	Hollow fiber (PE)	0.4	Synthetic	8	9	2.5–5	[26]
Membrane	Flat sheet (PVDF)	0.22	COD: 10,213 mg/L	–	50	–	[27]
Mesh filter	Flat sheet (nylon)	–	Synthetic	9.2–9.3 1.6	10 50	2.6–4.5	[28]
Ash filter	Flat sheet	–	Synthetic	9.2–9.3	16.7	2.6–4.5	[28]
Mesh filter	Flat sheet (nylon)	30	Distillery spent wash (COD: 30,200–40,000 mg/L)	10–12	3.9 14	2.6 4.5	[29]
Mesh filter	Flat sheet (polyester)	30	Synthetic municipal wastewater	6–8	74–81	0.13–1.6	This study

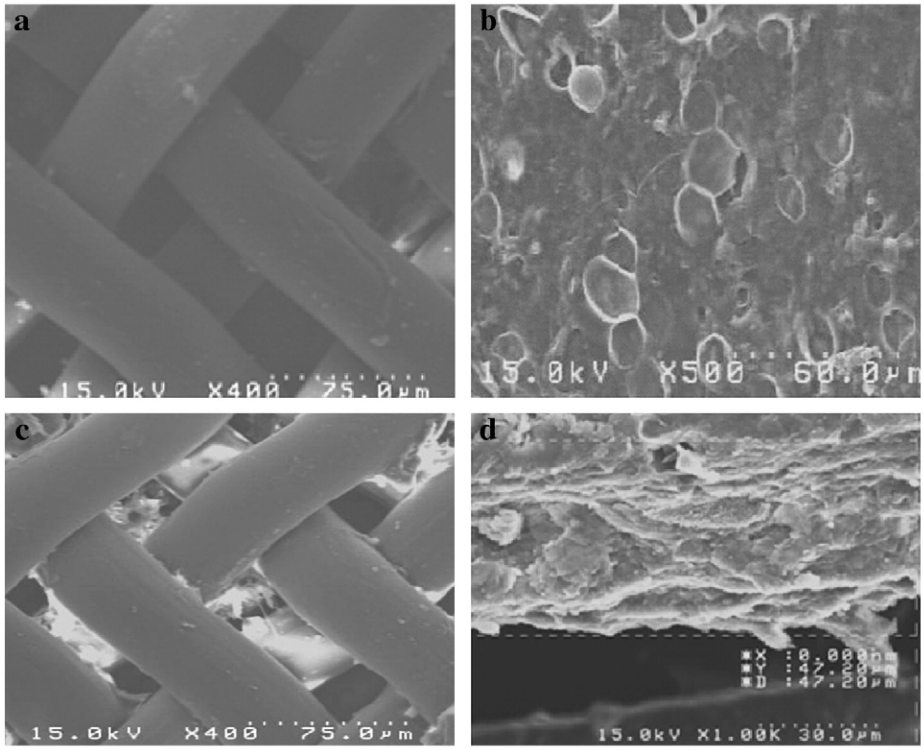

Fig. 6. SEM images: (a) fresh mesh filter, (b) cake layer, (c) pore blockage and (d) cross-section of cake layer.

operating conditions [31]. In this work, the deposition of sludge flocs onto the mesh surface and the attachment of the colloids and solutes between warp and weft fabrics are visualized by using SEM technique. The provided images are shown in Fig. 6. The periodic inspection of module during experiment runs shows that the cake layer is not uniformly extended on the entire surface of the filter fibers and the separate slices of the cake are locally formed at the filter surface. It is attributed to the inhomogeneous flow distribution between pores that leads to the progressive closure of pores. Consequently, the cake layer is only formed at the regions of the filter that have been already obstructed by the initial deposit in the filter pore [32]. The non-uniformity in the cake formation is more remarkable for the imposed flux 80 LMH in comparison with other sub-critical fluxes. This phenomenon has been previously reported for membrane medium [33]. To identify the main contributor to filtration resistance for each point depicted in Fig. 7, the hydraulic resistance analysis is conducted according to the resistance-in-series model as before described. The intrinsic filter resistance (R_m) value is around 7.9×10^8 m^{-1}, which does not change with increase of operation time. The filtration resistances are quantitatively measured for the imposed fluxes of 30 and 80 LMH at all points 1–5. As shown in Fig. 7, the intrinsic filter resistance (R_m) and the fouling resistance (R_f) lead to be minor contributors to the total resistance (R_t). The biological cake resistance (R_c), however, is a major factor of the total resistance. Furthermore, the fraction of bio-cake resistance to the total resistance increases steadily when the TFP increases. From points 1 to 3 (flux = 30 LMH) and points 4 to 5 (flux = 80 LMH), the fraction of bio-cake resistance to the total resistance increases from 0.77 to 0.92. At the final stage of filtration for two imposed fluxes (point 3 and point 5), the R_c values reach more than 90% and 92% of the total filtration resistance, respectively. This finding indicates that the value of R_c caused by the formation of the bio-cake on the filter surface is mainly responsible for the increase in TFP. The total resistance for the polyester mesh filter is in the range of 9.15×10^{11} to 1.2×10^{12} m^{-1} for sub and super-critical flux, which is nearly similar to the resistance values reported in the previous studies for mesh media [13,28].

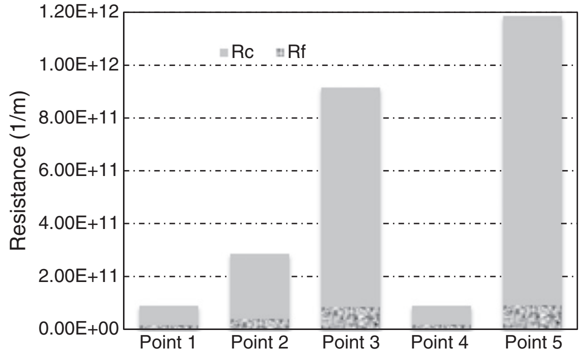

Fig. 7. Resistances through mesh filter and bio-cake at the corresponding points in Fig. 5.

3.4. Effect of aeration intensity

3.4.1. Suspended solid rejection and turbidity

The effect of the aeration intensity on the filtrate quality is investigated. The first stage, a tentative run is performed for monitoring the turbidity of filtrate of standard polymeric solution, Formazin suspension, prepared according to ASTM standard method for turbidity [34]. In this case, turbidity of the effluent reaches 95 NTU when the initial turbidity of Formazin suspension is 125 NTU. Suspended solid concentration and turbidity of the filtrate are monitored for the initial duration of 80 min under different values of SAD_m. Figs. 8 and 9, show the variations of filtrate quality as well as suspended solid and turbidity where the imposed flux is 30 LMH. In the case of SAD_m 0.5 m^3/m^2 h, a rather clear filtrate, less than 18 NTU of turbidity, is obtained in only 20 min and after that the turbidity of filtrate reaches 14 NTU and becomes constant. The filtrate quality is decreased when the aeration rate increases. Low aeration rate leads to stable formation of

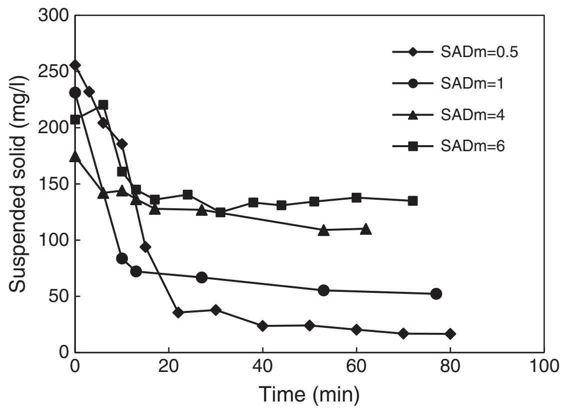

Fig. 8. The variations of suspended solids of filtrate against filtration time at different values of SAD_m.

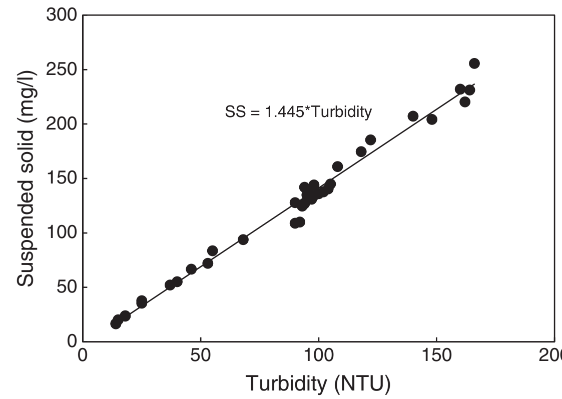

Fig. 10. Relationship between suspended solid and turbidity.

cake layer so called dynamic membrane and thus better SS retention and filtrate quality. In addition to aeration rate, the place of sparger can affect the filtrate quality. To indicate the effect of sparger arrangement on the filtrate quality, two experiment runs are performed at constant SAD_m 0.5 m^3/m^2 h. The first run is done when a pipe sparger, directly placed under the filter module, is set off and second run is carried out when pipe sparger below the filter module is set on. It is observed that a turbid effluent is achieved when the pipe sparger below the filter module is set on. Thus, it is essential to create somewhat moderate flow conditions in close proximity to the surface of mesh filter. The results also show that turbidity and suspended solid of the filtrate are highly correlated, with 1 turbidity unit corresponding to 1.44 mg/L suspended solid as shown in Fig. 10.

3.4.2. Filtration resistance

Air sparging in a MBR system has two contradictory impacts with regards to membrane fouling alleviation. Higher rates of aeration expeditiously remove the foulant layer formed at the membrane surface and simultaneously lead to the breakage of microbial flocs that causes the release of macromolecule polymeric substances [35,36]. The effect of aeration intensity on the filtration resistance has been investigated. As shown in Fig. 11, at the imposed fluxes lower than the measured critical flux, the filtration resistance decreases with increasing aeration intensity. However, a lower variation for the filtration resistance is obtained for the imposed flux 60 LMH. For the imposed flux 80 LMH, a different effect of the aeration intensity on the filtration performances is observed. The filtration resistance is not significantly decreased by increasing the intensity of aeration. It may be attributed to the fact that the drag force, acted on the cake layer, overcomes the shear force generated by the air bubbling [37]. The acquired result also shows that the higher increase in aeration intensity causes the increase in the filtration resistance. It can be explained that the higher aeration intensity has a more detrimental effect on the suspended flocs by breaking them up into smaller particles, leading to the release of extracellular polymeric substances into the supernatant to a greater extent [38]. Moreover, with the vigorous turbulence generated by aeration, the larger particles deposited on the mesh become more susceptible to the back-transport. This phenomenon is responsible to the particles with the diameters ranging from 1 to 50 μm [39,40]. Consequently, the fractions of small particles and macro-organic matter selectively deposited on the mesh surface are increased, leading to the low porosity of bio-cake [41].

3.4.3. Zeta potential of biomass

Extracellular polymeric substances have an obvious influence on surface charge of sludge flocs and can be correlated with the zeta potential [42,43]. Thus, to identify the amount of polymeric substances in biomass, the zeta potential of sludge which reflects the surface charge of sludge flocs is measured. The zeta potential of sludge changes from −28 to −14 mV at different values of SAD_m as depicted in Fig. 11. As can be seen, when SAD_m value is lower than 2 m^3/m^2 h, the increase in aeration intensity does not decrease significantly the zeta potential. On the other hand, when SAD_m value is higher than 2 m^3/m^2 h, the increase in aeration rate increases negatively the zeta potential. As mentioned before, higher rates of aeration lead to the breakage of microbial flocs and thus a higher release of macromolecule polymeric substances occurs. Consequently, the release of extracellular polymeric substances decreases significantly the zeta potential of biomass. The variations of the zeta potential with the aeration rate can be substantial evidence to the alterations of the filtration resistance. Thus, an optimum aeration rate is obtained at SAD_m

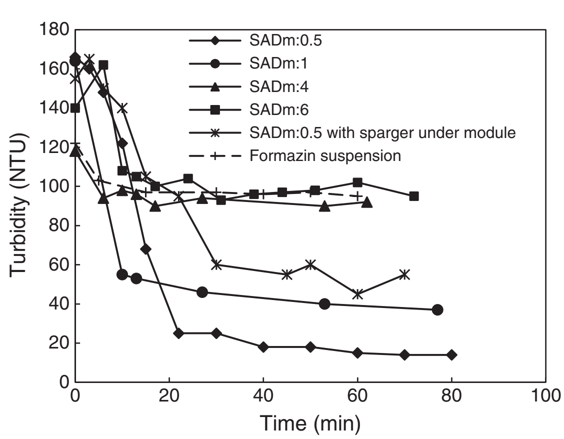

Fig. 9. The variations of filtrate turbidity against filtration time at different values of SAD_m.

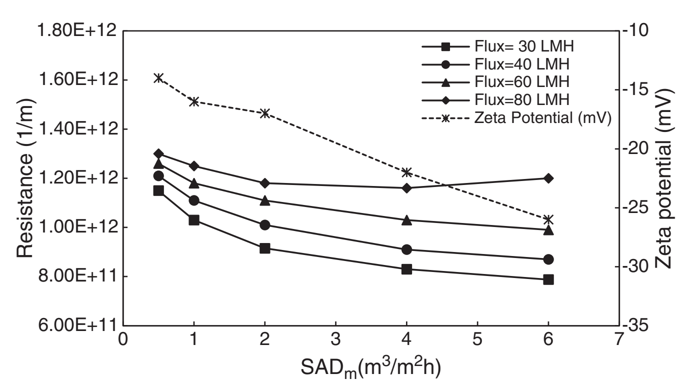

Fig. 11. The variations of filtration resistance and zeta potential against SAD_mat various imposed fluxes.

2 m^3/m^2 h beyond which a further increase in aeration rate has no effect on the resistance suppression. It has also been observed by Ueda et al. [35].

4. Conclusion

The critical flux of the mesh filter bioreactor is measured by using flux-step approach. The critical flux changes from 77 to 81 LMH when the SAD_m varies from 0.5 to 6 m^3/m^2 h. The long term operation of mesh filter bioreactor is performed at several imposed fluxes. At the imposed fluxes 30 and 40 LMH, the monofilament mesh establishes stable flux over the duration of 12 and 8 operating days, respectively. At the imposed flux 80 LMH, the TFP increases rigorously due to rapid accumulation of foulants and reaches 100 mbar during 8 h of filtration. The results obtained from resistance analysis show that the cake layer is a major factor of total resistance of mesh filtration. The value of cake resistance reaches more than 80% of total filtration resistance. The filtrate quality decreases with increasing aeration intensity. Turbidity of the filtrate reaches about 14 and 100 NTU for SAD_m 0.5 and 6 m^3/m^2 h, respectively. The filtration resistance decreases with increasing aeration intensity at sub-critical flux. At super-critical flux, the filtration resistance decreases slightly with increasing aeration rate until SAD_m 2 m^3/m^2 h and thereafter increases. Zeta potential of biomass decreases slightly for SAD_m value less than 2 m^3/m^2 h and declines severely for SAD_m value more than 2 m^3/m^2 h. There is an optimum SAD_m, 2 m^3/m^2 h, beyond which there is no further effect on the filtration resistance suppression.

The results point out that higher aeration intensity decreases the particulate separation characteristics while lower aeration intensity leads to increasing the filtration resistance of the mesh. The optimal aeration intensity improves the filtration performance because of two following reasons: 1) to form stable dynamic membrane and 2) to prevent the excess accumulation of sludge on the mesh surface.

Acknowledgment

The authors would like to thank Iranian National Petrochemical Company (NPC), Department of Health, Safety and Environment (HSE), for supporting the project.

References

[1] J.A. Howell, H.C. Chua, T.C. Amot, In situ manipulation of critical flux in a submerged membrane bioreactor using variable aeration rates and effects of membrane history, J. Membr. Sci. 242 (2004) 13–19.
[2] E.J. McAdam, S.J. Judd, A review of membrane bioreactor potential for nitrate removal from drinking water, Desalination 196 (2006) 135–148.
[3] K. Brindle, T. Stephenson, The application of membrane biological reactors for the treatment of wastewaters, Biotechnol. Bioeng. 49 (1996) 601–610.
[4] C. Visvanathan, R. Ben-Aim, K. Parameshwaran, Membrane separation bioreactors for wastewater treatment, Crit. Rev. Environ. Sci. Technol. 30 (2000) 1–48.
[5] B. Marrot, A. Barrios-Martinez, P. Moulin, N. Roche, Industrial wastewater treatment in a membrane bioreactor: a review, Environ. Prog. 23 (2004) 59–68.
[6] S. Rosenberger, M. Kraume, Filterability of activated sludge in membrane bioreactors, Desalination 151 (2003) 195–200.
[7] T. Stephenson, S. Judd, B. Jefferson, K. Brindle, Membrane Bioreactors for Wastewater Treatment, IWA Publishing, London, 2000.
[8] P. Le-Clech, V. Chen, T.A.G. Fane, Fouling in membrane bioreactors used in wastewater treatment, J. Membr. Sci. 284 (2006) 17–53.
[9] F. Meng, S.R. Chae, A. Drews, M. Kraume, H.-S. Shin, F. Yang, Recent advances in membrane bioreactors (MBRs): membrane fouling and membrane material, Water Res. 43 (2009) 1489–1512.
[10] Y. Kiso, Y.J. Jung, T. Ichinari, M. Park, T. Kito, K. Nishimura, K.S. Min, Wastewater treatment performance of a filtration bio-reactor equipped with a mesh as a filter material, Water Res. 17 (2000) 4143–4150.
[11] Y. Kiso, Y.J. Jung, T. Ichinari, M. Park, T. Kito, K. Nishimura, K.S. Min, Coupling of sequencing batch reactor and mesh filtration: operational parameters and wastewater treatment performance, Water Res. 39 (2005) 4887–4898.
[12] W. Fuchs, C. Resch, M. Kernstock, M. Mayer, P. Schoeberl, R. Braun, Influence of operational conditions on the performance of a mesh filter activated sludge process, Water Res. 39 (2005) 803–810.
[13] M.C. Chang, R.Y. Horng, H. Shao, Y.J. Hu, Performance and filtration characteristics of non-woven membranes used in a submerged membrane bioreactor for synthetic wastewater treatment, Desalination 191 (2006) 8–15.
[14] X. Ren, H.K. Shon, N. Jang, Y.G. Lee, M. Bae, J. Lee, K. Cho, I.S. kim, Novel membrane bioreactor (MBR) coupled with a nonwoven fabric filter for household wastewater, Water Res. 44 (2010) 751–760.
[15] W.M. Zahid, S.A. El-shafai, Use of cloth-media filter for membrane bioreactor treating municipal wastewater, Bioresour. Technol. 102 (2011) 2193–2198.
[16] Standard Methods for the Examination of Water and Wastewater, 20th ed. American Public Health Association/American Water Works Asso-ciation/Water Environment Federation, Washington, DC, USA, 1999.
[17] I.S. Chang, C.H. Lee, Membrane filtration characteristics in membrane-coupled activated sludge system — the effect of physiological states of activated sludge on membrane fouling, Desalination 120 (1998) 221–233.
[18] M. Mulder, Basic Principles of Membrane Technology, Kluwer Academic Publisher, 1996.
[19] M. Cheryan, Ultrafiltration and Microfiltration Handbook, Technimic Publishing, 1998.
[20] J.M. Lee, W.Y. Ahn, C.H. Lee, Comparison of the filtration characteristics between attached and suspended growth microorganisms in submerged membrane bioreactor, Water Res. 35 (2001) 2435–2445.
[21] R.W. Field, D. Wu, J.A. Howell, B.B. Gupta, Critical flux concept for microfiltration fouling, J. Membr. Sci. 100 (1995) 259–272.
[22] Z. Wu, Z. Wang, S. Huang, S. Mai, C. Yang, X. Wang, Z. Zhou, Effects of various factors on critical flux in submerged membrane bioreactors for municipal wastewater treatment, Sep. Purif. Technol. 62 (2008) 56–63.
[23] Z. Wang, Z. Wu, X. Yin, L. Tian, Membrane fouling in a submerged membrane bioreactor (MBR) under sub-critical flux operation: membrane foulant and gel layer characterization, J. Membr. Sci. 325 (2008) 238–244.
[24] B.K. Hwang, W.N. Lee, K.M. Yeon, P.K. Park, C.H. Lee, I.S. Chang, A. Drews, M. Kraume, Correlating TMP increases with microbial characteristics in the bio-cake on the membrane surface in a membrane bioreactor, Environ. Sci. Technol. 42 (2008) 3963–3968.
[25] U. Metzger, P. Le-Clech, R.M. Stuetz, F.H. Frimmel, V. Chen, Characterization of polymeric fouling in membrane bioreactors and the effect of different filtration modes, J. Membr. Sci. 301 (2007) 180–189.
[26] F.I. Hai, K. Yamamoto, k. Fukushi, Different fouling modes of submerged hollow – fiber and flat – sheet membranes induced by high strength wastewater with concurrent biofouling, Desalination 180 (2005) 89–97.
[27] B.D. Cho, A.G. Fane, Fouling transients in nominally sub-critical flux operation of a membrane bioreactor, J. Membr. Sci. 209 (2002) 391–403.
[28] P.K. Tewari, R.K. Singh, V.S. Batra, M. Balakrishnan, Membrane bioreactor (MBR) for waste water treatment: filtration performance evaluation of low cost polymeric and ceramic membranes, Sep. Purif. Technol. 71 (2010) 200–204.
[29] Y. Satyawali, M. Balakrishnan, Treatment of distillery in a membrane bioreactor (MBR) equipped mesh filter, Sep. Purif. Technol. 63 (2008) 278–286.
[30] P. Bacchin, P. Aimar, V. Sanchez, Model for colloidal fouling of membranes, AICHE J. 41 (1995) 368–376.
[31] J. Lee, W.Y. Ahn, C.H. Lee, Comparison of filtration characteristics between attached and suspended growth microorganisms in submerged bioreactor, Water Res. 35 (2001) 2435–2445.
[32] C.C. Ho, A.L. Zydney, A combined pore blockage and cake filtration model for protein fouling during microfiltration, J. Colloid Interface Sci. 232 (2000) 389–399.
[33] H.P. Chu, X.Y. Hi, Membrane fouling in a membrane bioreactor (MBR): sludge cake formation and fouling characteristics, Biotechnol. Bioeng. 90 (2005) 323–331.
[34] Standard test method for turbidity of water, ASTM D 1889, 2000.
[35] T. Ueda, K. Hata, Y. Kikuaka, O. Senio, Effects of aeration on suction pressure in a submerged membrane bioreactor, Water Res. 31 (1997) 489–494.
[36] C. Wisniewaki, A. Grasmick, A.L. Cruz, Critical particle size in membrane bioreactors: case of a denitrifying bacterial suspension, J. Membr. Sci. 197 (2000) 141–150.
[37] G. Belfort, R.H. Davis, The behavior of suspensions and macromolecular solutions in cross-flow microfiltration, J. Membr. Sci. 96 (1994) 1–58.
[38] I. Ivanovic, T. Leiknes, Impact of aeration rates on particle colloidal fraction in the biofilm membrane bioreactor (BF MBR), Desalination 231 (2008) 182–190.
[39] F. Fan, H. Zhou, H. Husain, Identification of wastewater sludge characteristics to predict critical flux for membrane bioreactor processes, Water Res. 40 (2006) 205–212.
[40] F. Meng, H. Zhang, F. Yang, L. Liu, Characterization of cake layer in submerged membrane bioreactor, Environ. Sci. Technol. 41 (2007) 4065–4070.
[41] S.H. Hong, W.N. Lee, H.S. OH, K.M. Yeon, B.K. Hwang, C.H. Lee, I.S. Chang, S. Lee, The effects of intermittent aeration on the characteristics of bio-cake layers in a membrane bioreactor, Environ. Sci. Technol. 41 (2007) 6270–6276.
[42] F. Meng, H. Zhang, F. Yang, S. Zhang, Y. Li, X. Zhang, Identification of activated sludge properties affecting membrane fouling in submerged membrane bioreactors, Sep. Purif. Technol. 51 (2006) 95–103.
[43] M. Wil'en, B. Jin, P. Lant, The influence of key chemical constituents in activated sludge on surface and flocculating properties, Water Res. 37 (2003) 2127–2139.